EEG frequency band analysis in chronic neuropathic pain

A linear and nonlinear approach to classify pain severity

Zolezzi, Daniela M; Alonso-Valerdi, Luz María; Ibarra-Zarate, David I

Published in:
Computer Methods and Programs in Biomedicine

DOI (link to publication from Publisher):
10.1016/j.cmpb.2023.107349

Publication date:
2023

Document Version
Publisher's PDF, also known as Version of record

Computer Methods and Programs in Biomedicine 230 (2023) 107349

Contents lists available at ScienceDirect

Computer Methods and Programs in Biomedicine

journal homepage: www.elsevier.com/locate/cmpb

EEG frequency band analysis in chronic neuropathic pain: A linear and nonlinear approach to classify pain severity

Daniela M. Zolezzi[a,c,*], Luz María Alonso-Valerdi[a], David I. Ibarra-Zarate[b]

[a] Escuela de Ingeniería y Ciencias, Tecnológico de Monterrey, Monterrey, Nuevo León 64849, Mexico
[b] Escuela de Ingeniería y Ciencias, Tecnológico de Monterrey, Vía Atlixcáyotl 2301, Puebla 72453, Mexico
[c] Department of Health Science and Technology, Center for Neuroplasticity and Pain (CNAP), Aalborg University, Frederik Bajers Vej 7A 2-207, Aalborg East 9220, Denmark

ARTICLE INFO

Article history:
Received 17 June 2022
Revised 20 December 2022
Accepted 9 January 2023

Keywords:
Neuropathic pain
EEG
Classification
Absolute band power
Approximate entropy
Disease characterization

ABSTRACT

Background and objective: Chronic neuropathic pain (NP) is a chronic pain condition that severely impacts a patient's life. Pain management has proved to be inefficient due to a lack of a simple clinical tool that may identify and monitor NP. A low-cost, noninvasive tool that provides relevant information on NP is the electroencephalogram (EEG). However, the commonly used linear EEG features have proved to be limited in characterizing NP pathophysiology. This study sought to determine whether nonlinear EEG features such as approximate entropy (ApEn) would better differentiate pain severity than absolute band power.
Methods: A non-parametric statistical approach based on the Brief Pain Inventory (BPI), along with linear and nonlinear EEG features, is proposed in this study. For this purpose, thirty-six chronic NP patients were recruited, and 22 channels were registered. Additionally, a control database of 13 participants with no NP was used as a reference, where 19 channels were registered. For both groups, EEG was recorded for 10 min in a resting state: 5 min with eyes open (EO) and 5 min with eyes closed (EC). Absolute band power and ApEn EEG features in the five clinical frequency bands (delta, theta, alpha, beta, and gamma) were estimated for all channels in both groups. As a result, 220-dimensional and 190-dimensional feature vectors were obtained for experimental and control classes respectively. For the experimental class, NP patients were grouped according to their BPI evaluation in three groups: low, moderate, and high pain. Finally, feature vectors were compared between groups using Kruskal Wallis and post-hoc Dunn's tests.
Results: ApEn revealed significant statistical difference ($p <= 0.0001$) in most frequency bands and conditions among the groups. In contrast, power had less significant differences between groups, particularly with EO. Furthermore, NP groups were notably clustered using only ApEn in theta, alpha, and beta bands.
Conclusions: The results indicate that ApEn effectively characterizes the different severities of chronic NP rather than the commonly used linear features. ApEn and other nonlinear techniques (e.g., spectral entropy, Shannon entropy) might be a more suitable methodology to monitor chronic NP experience.

1. Introduction

Neuropathic pain (NP) is a direct consequence of a lesion or disease affecting the somatosensory system. NP is classified as chronic when its duration is longer than three months [1]. Throughout this course, the spinal cord and the brain respond with neuroplastic changes, which could progressively affect the quality of life of NP patients. Unfortunately, clinical pharmacological trials have failed to relieve pain effectively [2]. A reason might be the poor characterization and stratification of NP [2].

Furthermore, NP characterization has almost exclusively relied on subjective perception, which has hindered advances in clinical management [3]. The fundamental problem for characterization depends on the complexity of NP [4], given that neuroplasticity is dynamic and unpredictable. Nonetheless, the spontaneous component of NP has mainly been analyzed with linear methodologies using power as the standard technique to extract neurophysiological correlates from EEG signals [5–7]. The limitation of linear methods is that they assume a relatively simple behavior from the cerebral cortex. For instance, linearity assumes that the

Abbreviations: NP, Neuropathic Pain; EEG, Electroencephalogram; CNS, Central Nervous System; BPI, Brief Pain Inventory; PDQ, Pain Detect Questionnaire; ApEn, Approximate Entropy; EC, Eyes Closed; EO, Eyes Open.

* Corresponding author at: Department of Health Science and Technology, Center for Neuroplasticity and Pain (CNAP), Aalborg University, Selma Lagerlöfs Vej 249, 9260 Gistrup, Denmark.
E-mail address: dmz@hst.aau.dk (D.M. Zolezzi).

https://doi.org/10.1016/j.cmpb.2023.107349

respective output (i.e., the power amplitude from neuronal activity) is the sum of two or more inputs (i.e., the sum of action potentials of thousands of neurons). In some instances, however, the brain does not behave as a linear system. The dynamics of the brain constantly shift from complex (nonlinear systems) to predictable synchronicity (linear systems). This inherent shifting of neuronal dynamics is the most efficient way for the brain to detect changes in the internal and external environment while preserving its autonomous internal organization [8]. Some characteristic properties of complex systems can be observed in NP pathophysiology, such as (1) simple agents, (2) nonlinear interactions among components, (3) no central control, and (4) emergent behavior. Regarding the first property, neurons are simple relative to the system (i.e., CNS), and neurons are the principal agents of maladaptive plasticity, where changes include: an altered sensibility of receptors, ectopic generation of action potentials and reduced inhibition [9]. Second, nonlinear effects in NP emerge from amplifying and damping feedbacks and long-term depression of GABAergic interneurons [10], which have been proposed as a gateway for pain transmission to higher brain areas. In addition, synaptic connections between neurons are stochastic, meaning they may signal along a particular pathway once but not another [11]. Third, there is essentially no central control over the system because the components (i.e., neurons, neuronal networks, or frequency bands) control each other's activity.

Finally, neurons display emergent behavior in NP, which refers to the collective outcomes of the whole system which cannot be observed from a small group of neurons. When subject to NP, neurons have no predefined meaning: they specialize during the learning phase in an often unexpected manner [2]. Furthermore, emergent behavior displays a hierarchical organization in the perception of NP. In other words, a neuron cannot perceive pain. Perception is only possible from the collective dynamics of the system. Consequently, the pain percept emerges not as a direct one-to-one correlate of sensory input but as a dynamic state formed by various psychosocial factors (e.g., learning, expectation, affective state) [12]. In sum, considering the nonlinearity of NP, this study proposed to calculate the randomness of the brain measured with entropy in the EEG signals.

1.1. Related work

Pain classification has been sought in several studies without consistent results. Previous studies have focused on identifying the degree of pain sensitivity from EEG data of healthy subjects by inducing pain [13] and some have included nonlinear methods in their classifier [14–17]. In addition to the results of this classifier that were published elsewhere [17] and achieved 96% accuracy using a support vector machine, only two other studies have tried to differentiate three levels of pain [14,16]. They reached 88.67%, and 83% accuracy, respectively; one study [16] used fractal dimension, Shannon entropy, ApEn, and spectral entropy, whereas [14] used metrics from functional connectivity (including nonlinear features). Despite their performance, the computational demand for connectivity is exceptionally high, and of the 12 features extracted by [16] none of the features could discriminate between the three classes. Different types of entropy have been applied to characterize the chaotic behavior of the human system in time series data, such as approximate entropy (ApEn), sample entropy, and multiscale entropy. The development of ApEn was founded on limitations of data length and noise commonly found in EEG datasets [18]. In addition, ApEn detects underlying episodic behavior undetected by peak amplitudes and preserves order in composite systems [19]. Thus, ApEn was chosen because it has been proven to characterize pathological states in Alzheimer's [20], major depressive disorder [21] and epilepsy [22].

Moreover, EEG signals of chronic low back pain patients (where low back pain was not NP) had a significantly reduced ApEn in delta (1–3 Hz), theta (4–7 Hz), alpha (8–13 Hz), and beta (14–30 Hz) bands after a massage therapy [23]. Currently, there is no other nonlinear EEG analysis in patients with NP.

Based on the unpredictable pathophysiology of NP, the present study aimed to determine whether ApEn band features would provide a better characterization than the commonly used band power features by differentiating frequency bands between NP severities and a control group. In addition, the efficacy of both models of neuronal dynamics to characterize NP with an unsupervised method is explored in this study. Patients were stratified based on the severity of pain (low, moderate, and high) according to the Brief Pain Inventory (BPI) questionnaire.

2. Methods

2.1. Neuropathic pain patients dataset

Thirty-six patients suffering from chronic NP were recruited for this study. The resulting database is publicly available in [24]. For a patient-specific feature analysis, the complete details for all chronic NP patients are stated in Table 1. More information, such as inclusion and exclusion criteria, surgical or psychological treatment, and time with pharmacological treatment, are indicated in the repository files [24]. Sample size calculation was computed before the study (See supplementary data for details, Section 1). It was calculated that to have a power between 0.8 and 0.9, 32–43 patients with chronic NP were needed. Thirty-six chronic NP patients (8 men and 28 women) with a mean age of 44±13.98 were recruited. The questionnaires used in this study were Pain Detect Questionnaire (PDQ) and Brief Pain Inventory (BPI), both validated for the Spanish language [25,26]. To characterize the different neuronal dynamics by the severity of NP, the proposed stratification for the groups depended on the severity of pain marked in the "actual pain" question of the BPI. The PDQ and BPI actual pain scores are depicted in Fig. 1 and 2 of the Supplementary Material, Section 5. Three classes were considered: (a) low pain = 0–3, (b) moderate pain (Mod)= 4–6, and (c) high pain = 7–10. Table 2 shows the demographic characteristics of the three NP groups by severity. Before the experiment, all patients provided written informed consent according to the World Association Declaration of Helsinki. This study was approved by the Clinical Investigation Ethics Committee of Tecnológico de Monterrey (number: P000369-DN-RespElectro-CI-CR005).

2.2. Control sample dataset

For the control group, a database from the Hospital Universiti Sains Malaysia (HUSM), Kelantan, Malaysia [27] was used with 10 min EEG raw recordings of 13 individuals with no NP (mean age = 38.277 ± 15.64). The authors recorded 19 individuals in the complete dataset, of which 10 were women, and 9 were men. Due to missing data in the repository, only 13 subjects were successfully imported; thus, the exact number of men and women in this sample is unknown [28]. Control subjects were diagnosed as healthy condition after a psychiatric evaluation based on clinical questionnaires such as the Beck Depression Inventory-II (BDI-II) and Hospital Anxiety and Depression Scale (HADS) [28].

2.3. EEG recordings

The NP dataset includes 22 EEG channels (Fp1, Fp2, AFz, F7, F3, Fz, F4, F8, T7, C3, Cz, C4, T8, CPz, P7, P3, Pz, P4, P8, POz, O1, O2) with two earlobe references (M1 and M2) at a sampling rate of 250 Hz and a bandwidth of 0.1–100 Hz, recorded with the

Table 1
Dataset description for chronic NP patients.

ID	Age	Sex	Etiology of NP	Time with NP	Medical treatment for NP
0	25	F	Central Nervous System Disorder	More than 2 years	Pregabalin, Amitriptyline
1	57	F	Diabetes	More than 2 years	Tramadol
2	20	F	Painful peripheral neuropathy	More than 2 years	Ketorolac
3	34	F	Spinal cord or nerve root injury	More than 2 years	Tramadol
4	77	M	Spinal cord or nerve root injury	More than 2 years	None
5	51	F	Other (NP in the head and surrounding areas)	More than 2 years	None
6	42	M	Diabetes	3 - 6 months	Pentoxifylline, Diclofenac
7	23	F	Central Nervous System Disorder (CRPS or Lyme)	1 - 2 years	Gabapentin, Tramadol
8	58	F	Painful peripheral neuropathy	More than 2 years	Pregabalin, Gabapentin
9	24	M	Trigeminal neuralgia	More than 2 years	None
10	55	M	Diabetes	1 - 2 years	Pregabalin
11	48	M	Diabetes	More than 2 years	Gabapentin
13	50	F	Spinal cord or nerve root injury	More than 2 years	None
14	33	F	Spinal cord or nerve root injury	More than 2 years	Pregabalin, Tramadol, CBD derivatives, Acetaminophen
15	68	F	Painful peripheral neuropathy	1 - 2 years	Pregabalin, Tramadol
16	53	F	Other (NP irradiating from lower back, right arm, and left hip)	More than 2 years	Occasionally Ketorolac, mostly none
18	53	F	Diabetes	1 - 2 years	Acetaminophen
19	63	M	Diabetes	More than 2 years	Pregabalin
20	42	F	Spinal cord or nerve root injury	1 - 2 years	Pregabalin
21	27	F	Other (NP radiating from right hip to right glute and right leg)	More than 2 years	Tramadol, Methocarbamol
22	42	M	Spinal cord or nerve root injury	More than 2 years	CBD Derivatives
23	55	F	Trigeminal neuralgia	More than 2 years	Amitriptyline, Topiramate, Erenumab
24	32	M	Spinal cord or nerve root injury	6 months - 1 year	Pregabalin, Diclofenac
25	46	F	Spinal cord or nerve root injury	More than 2 years	Amitriptyline, Tramadol, Rivotril
26	60	F	Spinal cord or nerve root injury	More than 2 years	Gabapentin, Acemetacin
27	53	F	Painful peripheral neuropathy	More than 2 years	None
30	28	F	Painful peripheral neuropathy	6 months - 1 year	Amitriptyline
31	47	F	Spinal cord or nerve root injury	More than 2 years	Duloxetine
33	58	F	Painful peripheral neuropathy	More than 2 years	Occasionally Flanax or Robaxisal, mostly none
35	29	F	Painful peripheral neuropathy	More than 2 years	None
37	32	F	Trigeminal neuralgia	More than 2 years	None
38	50	F	Painful peripheral neuropathy	More than 2 years	Tramadol, Dexketoprofen
39	40	F	Central Nervous System Disorder*	More than 2 years	Pregabalin, CBD derivatives, rarely Ketamine
40	55	F	Painful peripheral neuropathy	More than 2 years	None
41	51	F	Painful peripheral neuropathy	More than 2 years	Occasionally Duloxine, mostly none
43	31	F	Spinal cord or nerve root injury	1 - 2 years	Occasionally CBD derivatives, mostly none

*Complex Regional Pain Syndrome or Lyme Disease.

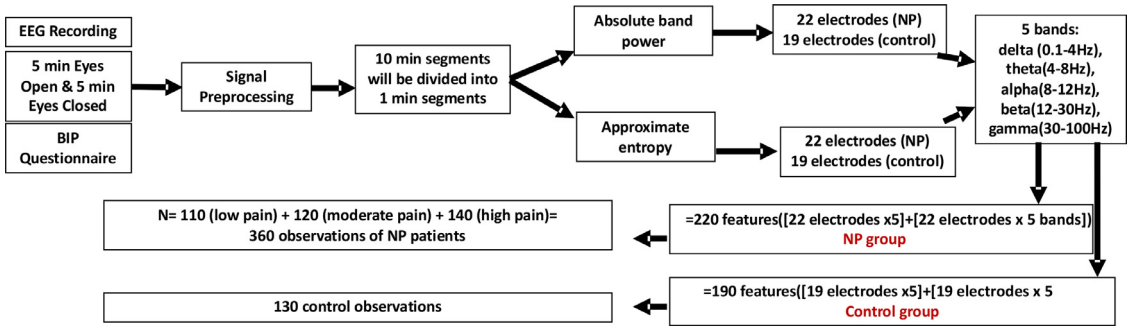

Fig. 1. Pipeline of signal analysis and feature extraction. The resulting feature vectors were: 220 × 360 for the NP group and 190 × 130 for the control group.

Table 2
Demographic characteristics for the three groups of chronic NP.

Group	Females	Males	Age
High pain	9	5	44.9 ± 14.6
Moderate pain	9	2	45.3 ± 13.8
Low pain	10	1	44.8 ± 14

mBrain amplifier. The control group dataset includes 19 EEG channels (Fp1, F3, C3, P3, O1, F7, T3, T5, Fz, Fp2, F4, C4, P4, O2, F8, T4, T6, Cz, and Pz) with standard link-ear (LE) reference, recorded with the Brain Discovery amplifier at 256 Hz and within a bandwidth of 0.1–100 Hz [28]. For both datasets, EEG recordings were conducted during eyes closed (EC) and eyes open (EO) conditions for 5 min each. During EO, participants were instructed to sit relaxed with minimum eye movements [28]. Several similarities validate the comparison between the control database and the chronic NP sample from this study: (1) age and sex were similar; (2) the recording conditions were 5 min EO and EC, (3) the sampling rate was 256 Hz, while for NP was 250 Hz, and (4) channel number (19 vs. 22) location (10/20 international system) and reference (earlobe) were comparable.

2.4. Data analysis

This section describes the signal analysis methods used for preprocessing, feature extraction, and data processing. All signal preprocessing and processing described below were performed in MATLAB R2020a (The Mathworks, Inc., Natick, MA, USA).

2.4.1. Preprocessing of raw EEG signals

Raw EEG signals were preprocessed using the EEGLAB toolbox (v.19.1.1) for MATLAB (R2020a) software. Signals were first filtered

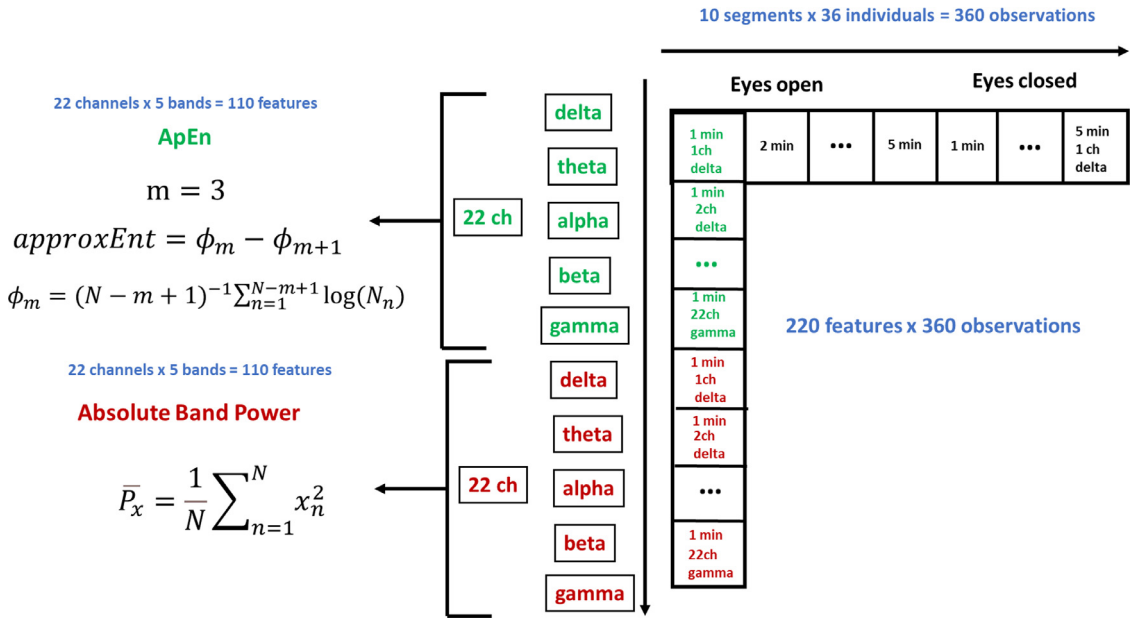

Fig. 2. Feature vector representation for chronic NP group. The first 110 features in the feature vector corresponded to the value of ApEn of 22 electrodes for each band, while the second 110 features corresponded to the value of absolute band power of 22 electrodes for each band. Each subject contributed to 10 observations.

at 0.1 Hz (6th-order Butterworth high-pass filter) to remove low-frequency artifacts. Then, transitory artifacts were rejected using the Artifact Subspace Reconstruction [29]. Muscular, ocular, cardiac, line noise or channel noise artifacts were removed by Independent Component Analysis supported by ICLabel [30]. Five filters were designed to filter segments into five clinical bands. The filters were 8th-order Butterworth bandpass filters with lower and higher frequencies of each band specified in the following section.

2.4.2. Feature extraction

A linear and nonlinear method were applied to estimate the dynamics in neuronal frequency bands, as illustrated in Fig. 1. All functions and programs used in this study are available for download [31]. The *Main.m* function in [31] calls each subject according to ID number and applies the custom-made function *FeatureExtraction_NP.m* (e.g., for the NP group), where features are extracted and returned to the main program to be stored in the main features vector. Of note, EEG signals were divided into 1 min segments before feature estimation, as seen in Algorithms 1 and 2. Features from 1 min segments might be more representative of the NP state, given the variability of brain signals. Subsequently, ApEn and absolute band power were estimated per segment for the 22 electrodes for five frequency bands: delta (0.1–4 Hz), theta (4–8 Hz), alpha (8–12 Hz), beta (12–30 Hz), and gamma (30–100 Hz).

2.4.3. Linear computation: absolute band power

Based on previous literature, the first feature chosen to study neuronal dynamics was absolute band power [5,6,32,33]. Absolute

Algorithm 1
Absolute Power per Frequency Band Algorithm for Chronic NP sample.

```
% *** Absolute Power per Frequency Band ***
% – Power per band and electrodes
power=zeros(110,10);%110 corresponds 5 bands x22 electrodes and 10 segments
1) Segment the signal in 1-minute segments
start=(5*fs):(fs*60):length(signals);
minute=(60*fs);
2) Position of the vector for every band – 22 electrodes
delta_pwr=1:22;
..
gamma_pwr=89:110;
3) For each filtered signal in the specific band, compute the absolute band power for each electrode
for i = 1:10
    fin = start(i)+minute;%Itinerate on the same electrode for every segment
    if i == 10% When segment = 10, next channel is computed
    fin = length(signals);
    end
    power(delta_pwr,i)=mean((ldelta(:,(start(i):fin))).^2,2);
    disp('delta')
4) After 22nd electrode, next frequency band starts itinerating
    ...
    power(gamma_pwr,i)=mean((lgamma(:,(start(i):fin))).^2,2);
disp('gamma')
end
4) Save power features in the individual subject vector to later export in general features vector
individual(111:end,:) = power;
end
```

Algorithm 2
Approximate entropy computation algorithm.

```
function [ap_total,i]=ENTROPY(a)
%Function with only one output: the ApEn of the signal in each channel.
1) IMPORTANT: Signal must be preprocessed
elag_total=[];
2) Dimension was defined before iterating
dim = 3;
for i = 1:22%22 channels for chronic NP
3) Lag is computed for every channel and condition
[~,lag] = phaseSpaceReconstruction(a(i,:),[],dim);
elag_total=[elag_total lag];
end
ap_total = [];
for i = 1:22%22 channels for chronic NP
4) ApEn is computed with dim=3, the previously calculated lag, and the tolerance factor r (0.2*variance(x)), which is the default in the function
    ap=approximateEntropy(a(i,:),elag_total(i),dim);
    ap_total= [ap_total ap];
end
end
```

band power was calculated to estimate the level of neuronal synchrony according to the Eq. (1),

$$\overline{P_x} = \frac{1}{N}\sum_{n=1}^{N} x_n^2 \tag{1}$$

where n refers to each sample of the signal x, N is the total number of samples of the signal x, and $\overline{P_x}$ is the mean power of the signal x. Absolute band power was extracted per frequency band using two custom-made functions, *FeatureExtraction_NP.m* (for NP group) and *FeatureExtraction_control.m* (control group) [31]. The section for the computation of absolute band power of this function is displayed in Algorithm 1.

2.4.4. Nonlinear computation: ApEN algorithm

ApEn quantifies the randomness in a time series, by measuring the likelihood that runs of patterns close to m observations remain close to the subsequent incremental comparisons. The signal is more predictable if more repetitive patterns are detected. As a result, ApEn yields a value from 0 to 2, where 2 corresponds to a random time series and 0 to a perfectly regular time series [34]. The custom-made function ENTROPY used for computing ApEn in this study is available [31] and it is shown in Algorithm 2.

As seen in Algorithm 2, before the computation of ApEn, three input parameters must be defined: m (i.e., the pattern length), lag τ (i.e., the delay), and the tolerance factor or tuning parameter r (i.e., similarity criterion). First, the dimension m was calculated using the False Nearest Neighbor algorithm [35]. The dimension was $m = 3$ for the control group and NP patients for EO and EC in most channels. Previous references held that the EO condition has an increased dimension than EC [36], but it was not the case for this study. The optimal number of previous values used to predict the subsequent value m depends on the number of data points [37]. Nonetheless, the value for m is typically chosen as $m = 2$ or $m = 3$, which follows the theoretical implications of [38].

Second, the lag τ was calculated for each channel and condition using the Average Mutual Information algorithm [39]. Notably, if the lag is too small, the state vectors would be reconstructed from lagging on nearly identical data points. Third, the number of within-range points at point n was calculated using Eq. (2):

$$N_n = \sum_{n=1, n\neq k}^{N} 1(\| Y_n - Y_k \|_\infty < R) \tag{2}$$

where 1 is the indicator function and R is the radius of similarity (r, the similarity criterion). The similarity criterion r was calculated as 0.2*variance(x), where x is the one-minute segment of a specific channel and subject in either EC or EO. These values have produced good statistical reproducibility for a time series of $N > 60$ [18]. In this way, ApEn calculates the logarithmic likelihood that the time series would repeat itself within the tolerance factor r both for m and for $m + 1$ samples. Finally, ApEn was calculated as $approxEnt = \phi_m - \phi_{m+1}$ in line with Eq. (3) using the Predictive Maintenance Toolbox [40],

$$\phi_m = (N - m + 1)^{-1} \sum_{n=1}^{N-m+1} \log(N_n) \tag{3}$$

where n refers to each sample of signal x, N is the total number of samples of N, and m is the segment of x wherefrom entropy is being calculated (see Algorithm 2).

2.4.5. Feature vectors

As a result, for the NP group, 220 features ([22 electrodes × 5 bands] + [22 electrodes × 5 bands]) were extracted, yielding 360 observations (36 patients × 10 EEG segments). For the control group, 190 features ([19 electrodes × 5 bands] + [19 electrodes × 5 bands]) were extracted, yielding 130 observations (13 patients × 10 EEG segments). This process has been summarized in Fig. 2, which provides a feature vector representation for this study. Before statistical analysis, data was normalized in the z-score scale with a center of 0 and a standard deviation of 1.

2.4.6. Statistical analysis

All computations for the statistical analysis were performed in RStudio (1.2.5033). ApEn and absolute band power from all electrodes and severities were grouped according to the EO and EC conditions from the resulting feature vectors. Second, a Shapiro-Wilk normality test was performed to test normality. ApEn and absolute band power estimates were non-normal; therefore, the non-parametric Kruskal Wallis test was applied for each band in EC and EO. Finally, Dunn's Kruskal-Wallis test was performed to compare the groups. See Supplementary Material for more details (Section 4).

3. Results

3.1. Statistical comparison by frequency bands

In this section, the ApEn of each electrode and the band power across regions are displayed in boxplots. Fig. 3 presents the delta, theta, and alpha band, and Fig. 4 illustrates the beta and gamma bands. Boxplots show the mean ApEn and absolute band power per severity level for each electrode (22 for NP and 19 for control)

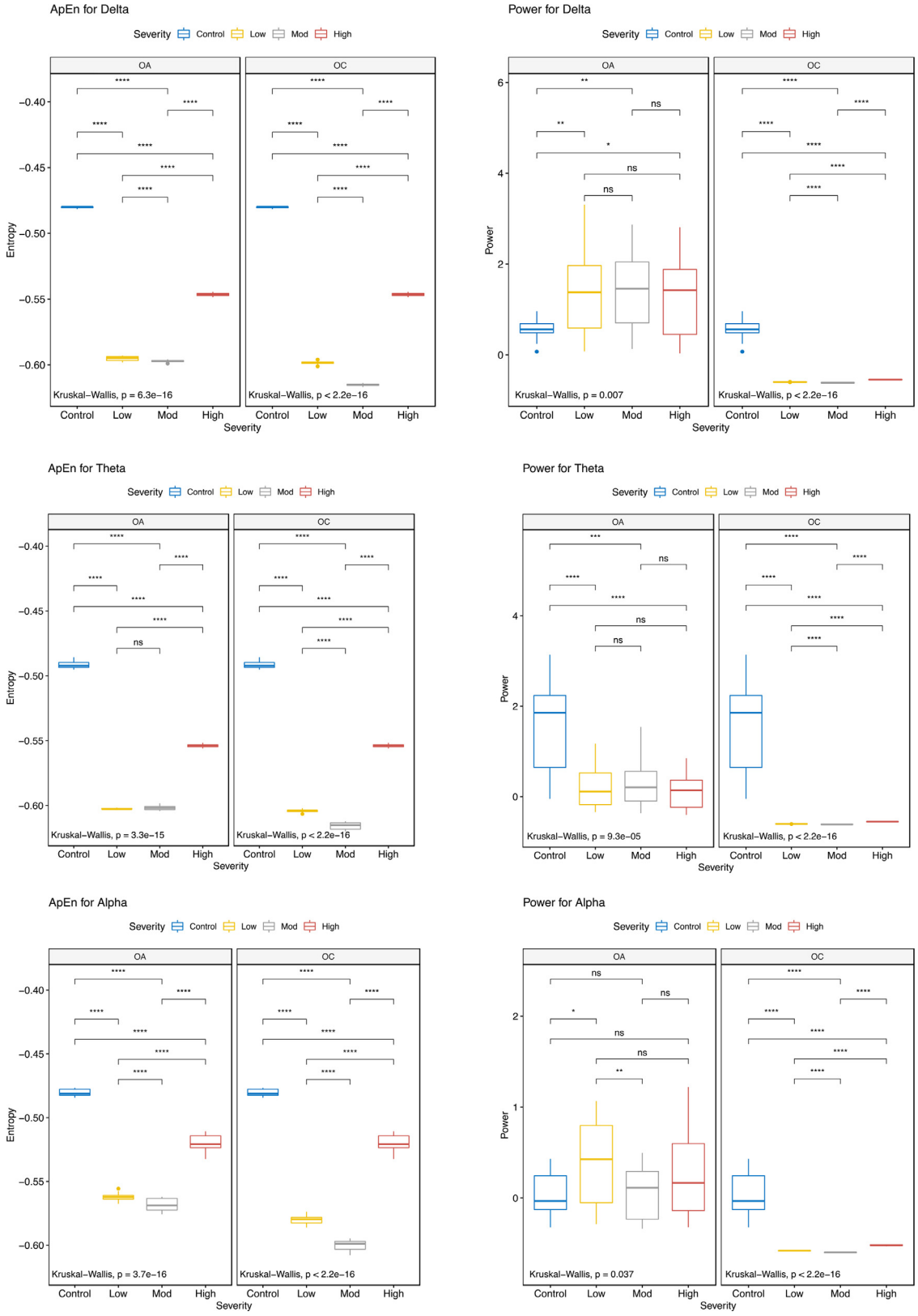

Fig. 3. Boxplots for ApEn and Power in delta, theta, and alpha band. ApEn in delta was most differentiable in EC, while only Low-Mod was insignificant in EO. For power, all groups showed a significant difference in EC, while for EO, only Control-Low and Control-Mod. For ApEn in theta EC, all groups showed a significant difference, while for EO, all groups except Low-Mod; in power EC, all groups were significant, whereas for EO, only Control-High, Control-Low, and Control-Mod. ApEn in alpha showed a significant difference for all groups in both conditions; in power, all groups in EC had a significant difference, while for EO, only Control-Low and Low-Mod. OA =Eyes Open, OC = Eyes Closed. Mod represents moderate severity. Circles over or under boxplots represent outliers. Data was normalized in a z-score scale with a center of 0 and a standard deviation of 1. Ns: $P > 0.05$, *: $P<=0.05$, **: $P<=0.01$, ***: $P<=0.001$, ****: $P<=0.0001$.

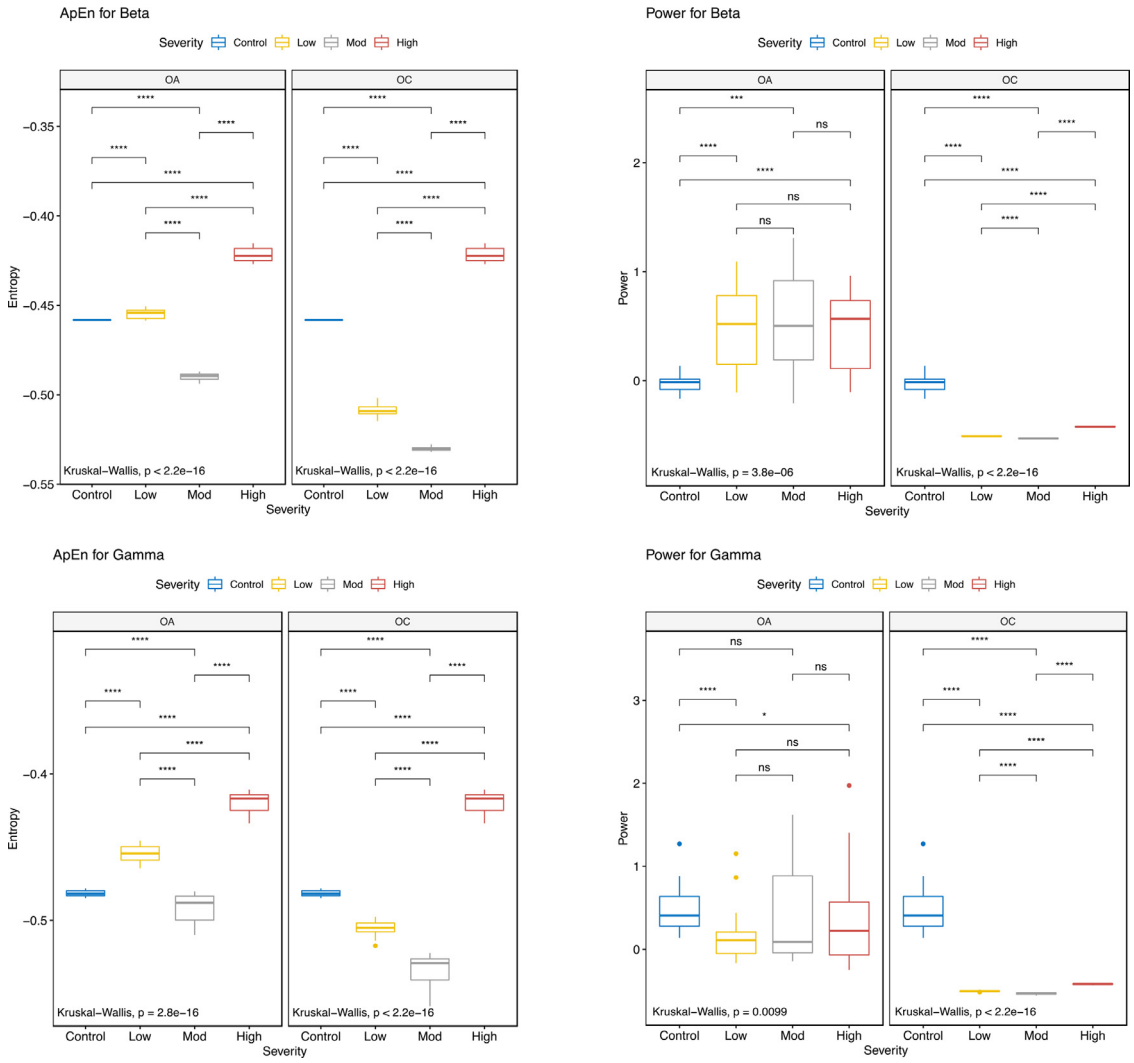

Fig. 4. Boxplots for ApEn and power in beta and gamma band. In beta ApEn all groups were significant in both EC and EO. For beta power in EO, only the control groups showed significant differences (Control-High, Control-Low, and Control-Mod), whereas, for EC, all groups were significant. In gamma ApEn, both conditions (EC and EO) had a significant difference for all groups. For power in EC, all groups were significant, but for EO, only Control-Low and Control-High. OA =Eyes Open, OC = Eyes Closed. Mod represents moderate severity. Circles over or under boxplots represent outliers. Data was normalized in a z-score scale with a center of 0 and a standard deviation of 1. Ns: $P > 0.05$, *: $P<=0.05$, **: $P<=0.01$, ***: $P<=0.001$, ****: $P<=0.0001$.

and each of the five frequency bands in both conditions. ApEn had overall significance in both conditions between the groups (EO and EC), while power had more non-significant groups in EO.

3.2. Topographical and spatial distribution of features

Given the significance of ApEn to significantly differentiate groups, theta (Fig. 5), alpha (Fig. 6), and beta (Fig. 7) bands are displayed topographically to visualize the changes between pain severity and state (EC and EO). In Fig. 8, scatterplots show an appropriate clustering for all groups in ApEn for both conditions.

4. Discussion

This study sought to determine whether nonlinear features would provide a better characterization than the commonly used linear features of EEG analysis for differentiating between NP severities, considering its unpredictable pathophysiology. In addition, to explore if neuronal frequency bands could characterize the same pathology with nonlinear analysis without the need for severity labels (i.e., as an unsupervised method). The results confirmed the relevance of ApEn as a nonlinear method that significantly differentiates most severities in both EO and EC. Furthermore, groups were clustered when the data was divided using only values of ApEn in theta, alpha, and beta (Fig. 8). The latter provides a preliminary foundation for exploring the application of unsupervised and supervised methods for monitoring NP with nonlinear features, especially ApEn. The nonlinear findings for each band will be discussed briefly concerning previous studies. The increased power of delta for the NP groups compared to the control group is in accordance with previous studies [6,32,33] and is related to the thalamocortical dysrhythmia mechanism, which enhances the amplitude of delta oscillations and serves as a means for the ongoing subconscious percept of pain [33]. ApEn could also differentiate NP severities in the theta band, as reported by others for power analysis in NP [6,41]. The slowing of the alpha band to theta band in NP patients is also driven by thalamocortical dysrhythmia [42]. This slowing may also explain the enhanced signal randomness in the theta band as pain severity increases, particularly in EC for moderate pain in the occipital lobe and the central and parietal electrodes for high pain (Fig. 5). Alpha has been reported previously as an “idling rhythm”, measuring the decrease in alpha power upon task performance. For instance, watching painful situations suppresses alpha oscillations in the somatosensory cortex

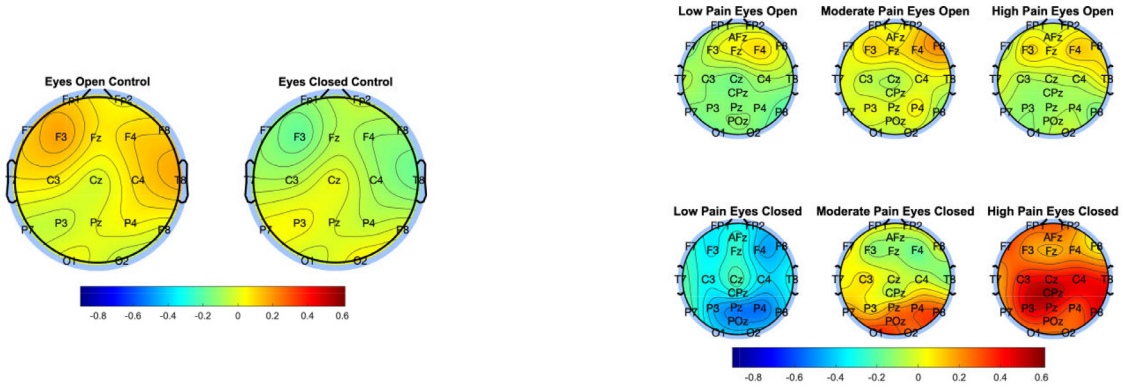

Fig. 5. ApEn for theta band in control and NP groups. There is increased ApEn for the control group in EO compared to EC. The slight increase of ApEn in the control group occurs over frontal and central electrodes bilaterally. Alternatively, the maximum changes for the NP group are observed in EC. There is decreased ApEn in low pain, whereas there is an enhanced ApEn in moderate pain for occipital (POz, O1, O2) and right parietal electrodes (Pz, P4, P8). High pain has a generalized enhanced ApEn as compared to other severities. Data was normalized in a z-score scale with a center of 0 and a standard deviation of 1. All groups were significantly different, ****: $P<=0.0001$.

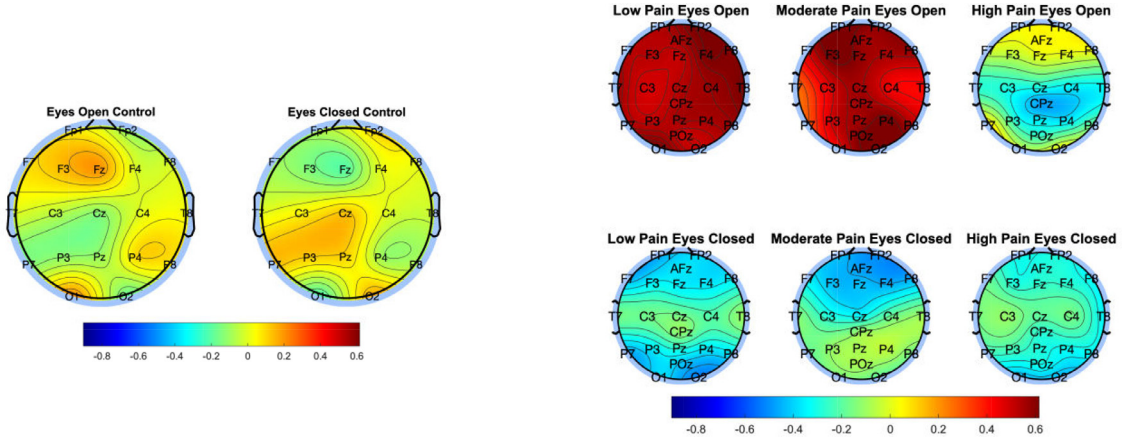

Fig. 6. ApEn for alpha band in control and NP groups. ApEn for the control group is enhanced in EO in some frontal (Fp1, F3, Fz), parietal (P3, P7, and P8), and occipital (O1) electrodes; in EC, increased ApEn is observed over left central (C3, Cz) and parietal (P7, P3, Pz) electrodes. Low and moderate pain in EO have a notable generalized increase in ApEn. High pain has a decreased ApEn for central and parietal electrodes (C3, Cz, C4, CPz, P3, Pz, P4). For all severities in EC, there is an overall decrease in ApEn compared to the control group. Data was normalized in a z-score scale with a center of 0 and a standard deviation of 1. All groups were significantly different, ****: $P<=0.0001$.

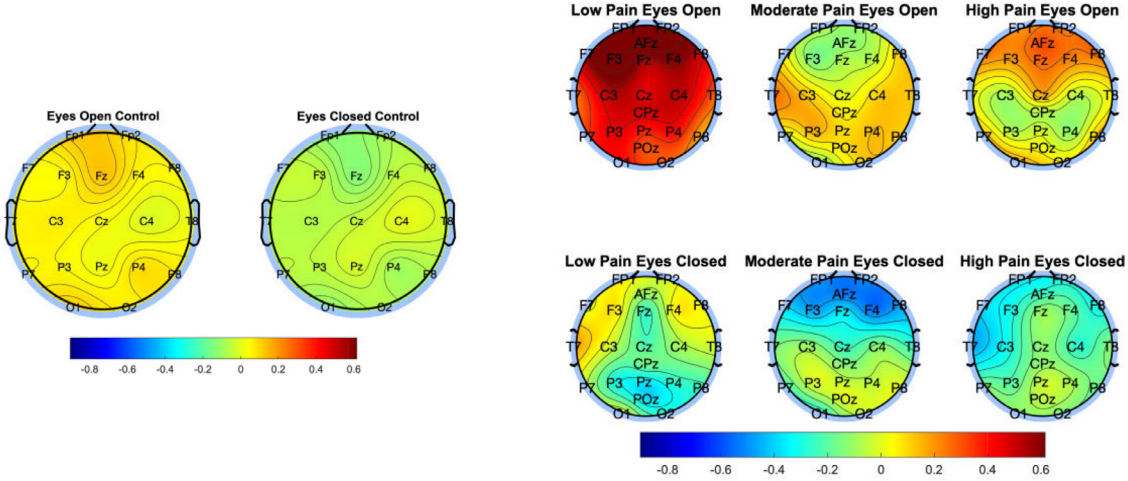

Fig. 7. ApEn for the beta band in the control and NP groups. Beta band for the control group showed an overall increase in ApEn in EO compared to EC. Similarly, ApEn was increased for all pain severities in EO. Relevantly, low and high pain in EO had an increased ApEn in the prefrontal (Fp1, Fp2, AFz) and frontal (F7, F3, Fz, F4, F8) electrodes. Moderate pain in EO slightly increases over temporal, parietal, and central electrodes. Moderate pain in EC slightly decreases ApEn in the prefrontal and frontal electrodes compared to the control group. Data was normalized in a z-score scale with a center of 0 and a standard deviation of 1. All groups were significantly different, ****: $P<=0.0001$.

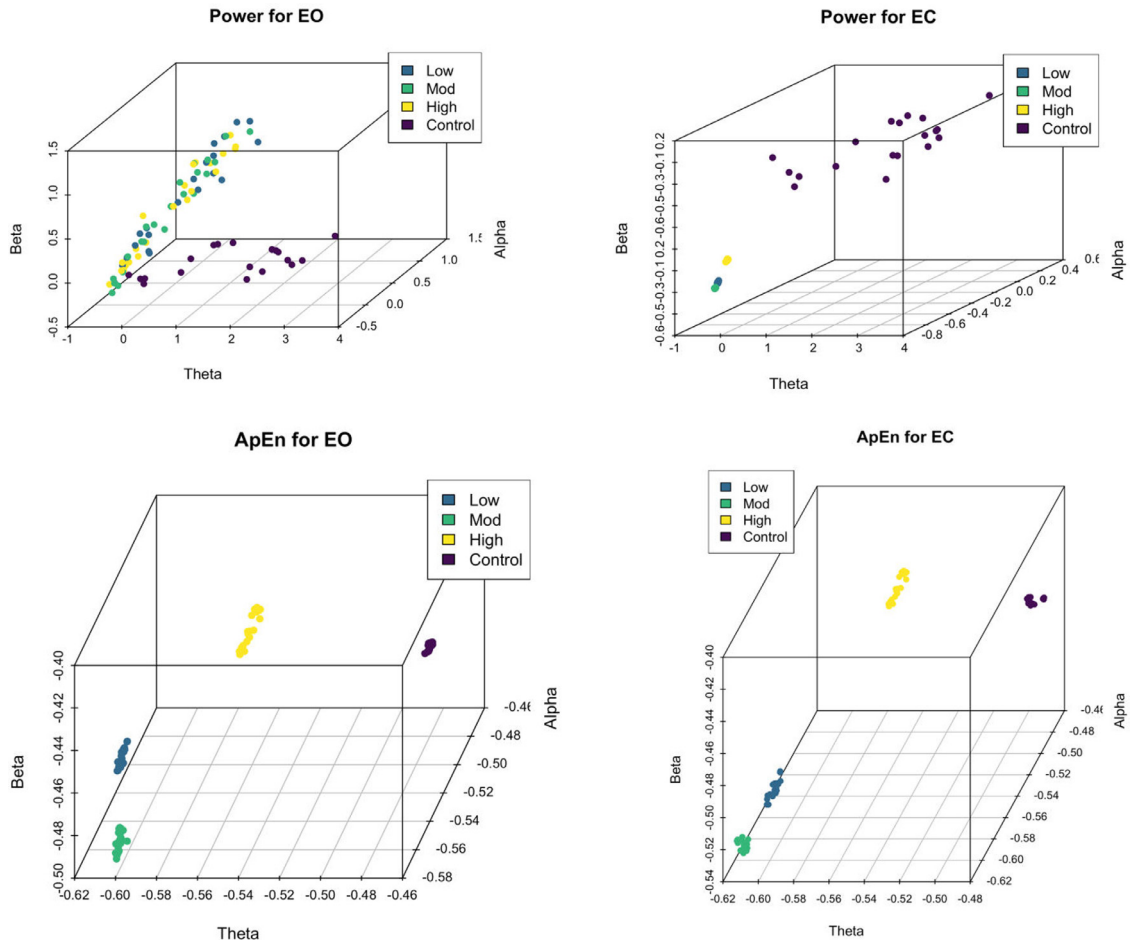

Fig. 8. 3D Spatial distribution of ApEn and power in theta, alpha, and beta band. ApEn clusters the 22 electrodes of NP severities and control group, whereas power does not. Data was normalized in a z-score scale with a center of 0 and a standard deviation of 1. Mod represents moderate severity.

[43]. Thus, attention toward constant NP may deactivate the cortex as if it were performing a task, suppressing alpha oscillations. Alternatively, alpha synchronization in the central/parietal region reflects top-down control during the perception of painful stimuli [44], whereas alpha desynchronization reflects the bottom-up release of this inhibitory control [45]. This increased desynchronization can be seen in the boxplots of Fig. 3 for EC, where power is decreased compared to the control group in the alpha band. There is also a substantial increase in randomness in NP (Fig. 6) for low and moderate pain. This enhanced randomness in the alpha band may reflect the bottom-up release of inhibitory control (desynchronization) and the allowance for the perception of NP. However, alpha has reduced randomness for high pain, which could reflect more top-down control or synchronization in high pain than in other pain severities. Also, the decreased power of NP severities in alpha could be attributed to lower attentional spans [46].

Beta is a prominent signal in the human sensorimotor cortex, correlated with GABA concentrations at rest as an index of pain [47]. Previous studies [5,32,33] report an increase in beta activity in neurogenic pain (i.e., NP) which is in line with the results of this study in EO. The lower beta power in EC (Fig. 4) may be explained by brain inhibition that is a consequence of deficiency of GABA, which leads to NP [48]. On the other hand, ApEn increased considerably for high pain severity compared to the other groups in both EC and EO, particularly for the frontal area (Fig. 7). This frontal relevance of beta supports previous results concerning the beta band in the frontal region as an optimal feature to predict central NP [5].

Conversely, lower gamma oscillations have been found in pain-relevant areas [49]. This lower activity in gamma oscillations can be observed in Fig. 4 for both EC and EO in power for the NP severities compared to the control state. However, for both conditions (EC and EO), high pain increased ApEn and power compared to the other NP severities. The latter supports the results of [50,51] which describe higher pain ratings associated with stronger frontal and prefrontal gamma oscillations. These results support the previous report on nonlinear features for classification [15], namely that nonlinear features might be more robust for disease identification than spectral domain features alone.

4.1. Limitations of the study and future directions

The limitations of this study are as follows. First, the study has a relatively small sample size. Second, other physiological processes that occur in the brain besides NP could also be responsible for the randomness observed in the EEG, including hemispheric differences [52] or alertness [53]. Third, despite the essential similarities between the control database and the recorded NP patients, the recording system was not the same, which could alter the signal recording quality. Fourth, the scatterplots show group clustering by using the mean of the segments in each electrode for every group, but the complete feature distribution would be needed to confirm patient-specific clustering. In addition, data for effective clustering and statistical differences were found given a long EEG recording for each state (5 min), which may not be optimal in clinical practice. Finally, although clinical history, pain specialist

criteria, and the PDQ were used to include patients with chronic NP, patients with widespread brain disorders (e.g., CRPS and Lyme disease) are not classified anymore as chronic NP in the updated International Classification of Diseases-11 (ICD-11)[1].

Nonetheless, these patients still have NP mechanisms and NP symptoms [54,55]. Thus, all patients that were included in this study had NP pathophysiology. Future work should address these limitations by (1) a larger sample size of NP patients and control participants, (2) an exploration of other nonlinear features (besides ApEn) that could cluster NP severities by using individual observations, (3) a study of nonlinear correlation in each of the bands between power and ApEn (since the residuals of the linear correlation were not normal), (4) the exploration of the minimum time required for an EEG recording to differentiate NP severities effectively.

5. Conclusion

The present study investigated the application of nonlinear features compared to linear features for the characterization of chronic NP. The results confirm the relevance of ApEn as a nonlinear method for EEG analysis that significantly differentiates control and chronic NP severities in both EO and EC. In addition, ApEn clusters NP severities without labels, proposing an alternative path for NP characterization using nonlinear methods. Although more studies in chronic NP are needed to confirm the efficacy of nonlinear analysis, this approach is promising in aiding clinicians and researchers in better pain management. This methodology could address the need for a simple clinical tool that may stratify chronic NP patients in clinical trials and develop pain experience monitoring systems in the clinical environment.

Ethical statement

This study was approved by the Clinical Investigation Ethics Committee of Tecnológico de Monterrey (P000369-DN-RespElectro-CI-CR005). The international standards compiled were in accordance with the World Association Declaration of Helsinki, International Conference of Harmonization ICH 96 (Guidelines for Ethical Committees), and the National Bioethics Advisory Committee 2001 for developing countries. As well as various national bioethical standards of Mexico, including the General Health Law in Matter of Research for Health (DOF 23 dic 1986).

Data availability statement

All raw EEG data from patients recorded in this study was published in the following database [24].

Declaration of Competing Interest

The authors do not have any conflicts of interest.

CRediT authorship contribution statement

Daniela M. Zolezzi: Investigation, Data curation, Formal analysis, Writing – original draft. **Luz María Alonso-Valerdi:** Supervision, Conceptualization, Software, Formal analysis, Validation, Writing – review & editing. **David I. Ibarra-Zarate:** Formal analysis, Supervision, Writing – review & editing.

Acknowledgments

Funding for this project was provided to DMZ by Consejo Nacional de Ciencia y Tecnología (CONACYT) (Grant No.: 1007725) and Tecnológico de Monterrey by granting a full tuition scholarship to DMZ. Special thanks to Dr. Fernando Cantú Flores from the Pain Management Center at Hospital Zambrano Hellion. The authors declare that they have no potential conflicts of interest. Center for Neuroplasticity and Pain (CNAP) is supported by the Danish National Research Foundation (DNRF121).

Supplementary materials

Supplementary material associated with this article can be found, in the online version, at doi:10.1016/j.cmpb.2023.107349.

References

[1] J. Scholz, N.B. Finnerup, N. Attal, Q. Aziz, R. Baron, M.I. Bennett, R. Benoliel, M. Cohen, G. Cruccu, K.D. Davis, S. Evers, M. First, M.A. Giamberardino, P. Hansson, S. Kaasa, B. Korwisi, E. Kosek, P. Lavand'Homme, M. Nicholas, T. Nurmikko, S. Perrot, S.N. Raja, A.S.C. Rice, M.C. Rowbotham, S. Schug, D.M. Simpson, B.H. Smith, P. Svensson, J.W.S. Vlaeyen, S.J. Wang, A. Barke, W. Rief, R.D. Treede, The IASP classification of chronic pain for ICD-11: chronic neuropathic pain, Pain 160 (2019) 53–59, doi:10.1097/j.pain.0000000000001365.

[2] N.B. Finnerup, S. Haroutounian, R. Baron, R.H. Dworkin, I. Gilron, M. Haanpaa, T.S. Jensen, P.R. Kamerman, E. McNicol, A. Moore, S.N. Raja, N.T. Andersen, E.S. Sena, B.H. Smith, A.S.C. Rice, N. Attal, Neuropathic pain clinical trials, Pain 159 (2018) 2339–2346, doi:10.1097/j.pain.0000000000001340.

[3] K. Bannister, J. Sachau, R. Baron, A.H. Dickenson, Neuropathic pain: mechanism-based therapeutics, Annu. Rev. Pharmacol. Toxicol. 60 (2020) 257–274, doi:10.1146/annurev-pharmtox-010818-021524.

[4] D.M. Zolezzi, L.M. Alonso-Valerdi, D.I. Ibarra-Zarate, Chronic neuropathic pain is more than a perception: systems and methods for an integral characterization, Neurosci. Biobehav. Rev. 136 (2022) 104599, doi:10.1016/j.neubiorev.2022.104599.

[5] A. Vuckovic, V.J.F. Gallardo, M. Jarjees, M. Fraser, M. Purcell, Prediction of central neuropathic pain in spinal cord injury based on EEG classifier, Clin. Neurophysiol. (2018), doi:10.1016/j.clinph.2018.04.750.

[6] P. Boord, P.J. Siddall, Y. Tran, D. Herbert, J. Middleton, A. Craig, Electroencephalographic slowing and reduced reactivity in neuropathic pain following spinal cord injury, Spinal Cord 46 (2008) 118–123, doi:10.1038/sj.sc.3102077.

[7] M. Ploner, C. Sorg, J. Gross, Brain rhythms of pain, Trends Cogn. Sci. (2017), doi:10.1016/j.tics.2016.12.001.

[8] G. Buzsáki, Rhythms of the Brain, Oxford University Press, 2006, doi:10.1093/acprof:oso/9780195301069.001.0001.

[9] M. Costigan, J. Scholz, C.J. Woolf, Neuropathic pain: a maladaptive response of the nervous system to damage, Annu. Rev. Neurosci. (2009), doi:10.1146/annurev.neuro.051508.135531.

[10] Y.H. Kim, S.K. Back, A.J. Davies, H. Jeong, H.J. Jo, G. Chung, H.S. Na, Y.C. Bae, S.J. Kim, J.S. Kim, S.J. Jung, S.B. Oh, TRPV1 in GABAergic interneurons mediates neuropathic mechanical allodynia and disinhibition of the nociceptive circuitry in the spinal cord, Neuron 74 (2012) 640–647, doi:10.1016/j.neuron.2012.02.039.

[11] C. Körber, T. Kuner, Molecular machines regulating the release probability of synaptic vesicles at the active zone, Front. Synaptic Neurosci. 8 (2016), doi:10.3389/fnsyn.2016.00005.

[12] R. Kuner, T. Kuner, Cellular circuits in the brain and their modulation in acute and chronic pain, Physiol. Rev. 101 (2021) 213–258, doi:10.1152/physrev.00040.2019.

[13] E. Schulz, A. Zherdin, L. Tiemann, C. Plant, M. Ploner, Decoding an individual's sensitivity to pain from the multivariate analysis of EEG data, Cereb. Cortex 22 (2012) 1118–1123, doi:10.1093/cercor/bhr186.

[14] P. Modares-Haghighi, R. Boostani, M. Nami, S. Sanei, Quantification of pain severity using EEG-based functional connectivity, Biomed. Signal Process. Control 69 (2021) 102840, doi:10.1016/j.bspc.2021.102840.

[15] M. Vatankhah, V. Asadpour, R. Fazel-Rezai, Perceptual pain classification using ANFIS adapted RBF kernel support vector machine for therapeutic usage, Appl. Soft Comput. 13 (2013) 2537–2546, doi:10.1016/j.asoc.2012.11.032.

[16] T. Nezam, R. Boostani, V. Abootalebi, K. Rastegar, A novel classification strategy to distinguish five levels of pain using the EEG signal features, IEEE Trans. Affect Comput. 12 (2021) 131–140, doi:10.1109/TAFFC.2018.2851236.

[17] D.M. Zolezzi, L.M. Alonso-Valerdi, D.I. Ibarra-Zarate, N.E. Naal-Ruiz, D.M. Zolezzi, L.M. Alonso-Valerdi, N.E. Naal-Ruiz, D.I. Ibarra-Zarate, Identification of neuropathic pain severity based on linear and non-linear EEG features, in: Proceedings of the 43rd Annual International Conference of the IEEE Engineering in Medicine & Biology Society (EMBC), 2021, pp. 169–173, doi:10.1109/EMBC46164.2021.9630101.

[18] S. Pincus, Approximate entropy (ApEn) as a complexity measure, Chaos Interdiscip. J. Nonlinear Sci. 5 (1995) 110–117, doi:10.1063/1.166092.

[19] S.M. Pincus, Assessing serial irregularity and its implications for health, Ann. N Y Acad. Sci. (2001), doi:10.1111/j.1749-6632.2001.tb02755.x.

[20] D. Abásolo, R. Hornero, P. Espino, J. Poza, C.I. Sánchez, R.D. La Rosa, Analysis of regularity in the EEG background activity of Alzheimer's disease patients with approximate entropy, Clin. Neurophysiol. 116 (2005), doi:10.1016/j.clinph.2005.04.001.

[21] S.T. Chen, L.C. Ku, S.J. Chen, T.W. Shen, The changes of qEEG approximate entropy during test of variables of attention as a predictor of major depressive disorder, Brain Sci. 10 (2020) 828, doi:10.3390/brainsci10110828.
[22] V. Srinivasan, C. Eswaran, N. Sriraam, Approximate entropy-based epileptic EEG detection using artificial neural networks, IEEE Trans. Inf. Technol. Biomed. 11 (2007) 288–295, doi:10.1109/TITB.2006.884369.
[23] X. Sun, H. Li, W. Du, W. Chen, F. Zhou, L. Wang, Analysis of electroencephalogram of patients with specific low back pain with the massage treatment, in: Proceedings of the 39th Annual International Conference of the IEEE Engineering in Medicine and Biology Society (EMBC), IEEE, 2017, pp. 479–483, doi:10.1109/EMBC.2017.8036866.
[24] D.M. Zolezzi, N.E. Naal-Ruiz, L.M. Alonso-Valerdi, D.I. Ibarra-Zárate, Chronic Neuropathic Pain: EEG data in eyes open (5 min) and eyes closed (5 min) with questionnaire reports, Version 3, Mendeley Data Dataset. (2022), doi:10.17632/yj52xrfgtz.1.
[25] A.K. Erdemoglu, R. Koc, Brief pain Inventory score identifying and discriminating neuropathic and nociceptive pain, Acta Neurol. Scand. (2013), doi:10.1111/ane.12131.
[26] R. Freynhagen, R. Baron, U. Gockel, T.R. Tölle, painDETECT: a new screening questionnaire to identify neuropathic components in patients with back pain, Curr. Med. Res Opin (2006), doi:10.1185/030079906X132488.
[27] Mumtaz, Wajid; Malik, Aamir Saeed; Yasin, Mohd Azhar Mohd; Ali, Syed Saad Azhar; Xia, Likun (2016): EEG-based Diagnosis and Treatment Outcome Prediction for Major Depressive Disorder. figshare. Dataset. https://doi.org/10.6084/m9.figshare.3385168.v1
[28] W. Mumtaz, A.S. Malik, M.A.M. Yasin, L. Xia, Review on EEG and ERP predictive biomarkers for major depressive disorder, Biomed. Signal Process. Control 22 (2015) 85–98, doi:10.1016/J.BSPC.2015.07.003.
[29] M. Plechawska-Wojcik, M. Kaczorowska, D. Zapala, The Artifact Subspace Reconstruction (ASR) for EEG Signal Correction. A Comparative Study, 853, Springer, Cham, 2019, doi:10.1007/978-3-319-99996-8_1.
[30] L. Pion-Tonachini, K. Kreutz-Delgado, S. Makeig, ICLabel: an automated electroencephalographic independent component classifier, dataset, and website, NeuroImage (2019), doi:10.1016/j.neuroimage.2019.05.026.
[31] D.M. Zolezzi, L.M. Alonso-Valerdi; D.I. Ibarra-Zarate, Approximate entropy and absolute band power -frequency bands - file exchange - MATLAB central, (2022). MATLAB Scirpt. https://la.mathworks.com/matlabcentral/fileexchange/122267-approximate-entropy-and-absolute-band-power-frequency-bands (accessed December 18, 2022).
[32] J. Sarnthein, J. Stern, C. Aufenberg, V. Rousson, D. Jeanmonod, Increased EEG power and slowed dominant frequency in patients with neurogenic pain, Brain (2006), doi:10.1093/brain/awh631.
[33] J. Stern, D. Jeanmonod, J. Sarnthein, Persistent EEG overactivation in the cortical pain matrix of neurogenic pain patients, NeuroImage 31 (2006) 721–731, doi:10.1016/j.neuroimage.2005.12.042.
[34] L. Montesinos, R. Castaldo, L. Pecchia, On the use of approximate entropy and sample entropy with centre of pressure time-series, J. Neuroeng. Rehabil. 15 (2018), doi:10.1186/s12984-018-0465-9.
[35] C. Rhodes, M. Morari, False-nearest-neighbors algorithm and noise-corrupted time series, Phys. Rev. E Stat. Phys. Plasmas Fluids Relat. Interdiscip. Top. 55 (1997), doi:10.1103/PhysRevE.55.6162.
[36] W.S. Pritchard, D.W. Duke, Measuring chaos in the brain: a tutorial review of nonlinear dynamical EEG analysis, Int. J. Neurosci. 67 (1992), doi:10.3109/00207459208994774.
[37] A. Wolf, J.B. Swift, H.L. Swinney, J.A. Vastano, Determining Lyapunov exponents from a time series, Phys. D 16 (1985), doi:10.1016/0167-2789(85)90011-9.
[38] S.M. Pincus, I.M. Gladstone, R.A. Ehrenkranz, A regularity statistic for medical data analysis, J. Clin. Monit. 7 (1991), doi:10.1007/BF01619355.
[39] B. Kliková, A. Raidl, Reconstruction of phase space of dynamical systems using method of time delay, in: Proceedings of the 20th Annual Conference of Doctoral Students WDS, 2011.
[40] The MathWorks, Predictive Maintanence Toolbox (accessed 2021) Version 2.3 (Release 2021a). https://www.mathworks.com/help/predmaint/index.html.
[41] J. Sarnthein, D. Jeanmonod, High thalamocortical theta coherence in patients with neurogenic pain, NeuroImage (2008), doi:10.1016/j.neuroimage.2007.10.019.
[42] R.R. Llinás, U. Ribary, D. Jeanmonod, E. Kronberg, P.P. Mitra, Thalamocortical dysrhythmia: a neurological and neuropsychiatric syndrome characterized by magnetoencephalography, Proc. Natl. Acad. Sci. U. S. A. 96 (1999) 15222–15227, doi:10.1073/pnas.96.26.15222.
[43] Y. Cheng, C.Y. Yang, C.P. Lin, P.L. Lee, J. Decety, The perception of pain in others suppresses somatosensory oscillations: a magnetoencephalography study, NeuroImage 40 (2008) 1833–1840, doi:10.1016/j.neuroimage.2008.01.064.
[44] Y. Mu, Y. Fan, L. Mao, S. Han, Event-related theta and alpha oscillations mediate empathy for pain, Brain Res. 1234 (2008) 128–136, doi:10.1016/j.brainres.2008.07.113.
[45] W. Klimesch, P. Sauseng, S. Hanslmayr, EEG alpha oscillations: the inhibition-timing hypothesis, Brain Res. Rev. (2007), doi:10.1016/j.brainresrev.2006.06.003.
[46] M.S. Clayton, N. Yeung, R.C. Kadosh, The roles of cortical oscillations in sustained attention, Trends Cogn. Sci. (2015), doi:10.1016/j.tics.2015.02.004.
[47] T.J. Baumgarten, G. Oeltzschner, N. Hoogenboom, H.J. Wittsack, A. Schnitzler, J. Lange, Beta peak frequencies at rest correlate with endogenous GABA+/Cr concentrations in sensorimotor cortex areas, PLoS One 11 (2016) e0156829, doi:10.1371/journal.pone.0156829.
[48] P. Schwenkreis, A. Scherens, A.K. Rönnau, O. Höffken, M. Tegenthoff, C. Maier, Cortical disinhibition occurs in chronic neuropathic, but not in chronic nociceptive pain, BMC Neurosci. 11 (2010) 73, doi:10.1186/1471-2202-11-73.
[49] M.S. Barr, F. Farzan, K.D. Davis, P.B. Fitzgerald, Z.J. Daskalakis, Measuring GABAergic inhibitory activity with TMS-EEG and its potential clinical application for chronic pain, J. Neuroimmune Pharmacol. 8 (2013) 535–546, doi:10.1007/s11481-012-9383-y.
[50] R. Zhou, J. Wang, W. Qi, F.Y. Liu, M. Yi, H. Guo, Y. Wan, Elevated resting state gamma oscillatory activities in electroencephalogram of patients with postherpetic neuralgia, Front. Neurosci. 12 (2018), doi:10.3389/fnins.2018.00750.
[51] E.S. May, M.M. Nickel, S.T. Dinh, L. Tiemann, H. Heitmann, I. Voth, T.R. Tölle, J. Gross, M. Ploner, Prefrontal gamma oscillations reflect ongoing pain intensity in chronic back pain patients, Hum. Brain Mapp. 40 (2019) 293–305, doi:10.1002/hbm.24373.
[52] F. Alù, F. Miraglia, A. Orticoni, E. Judica, M. Cotelli, P.M. Rossini, F. Vecchio, Approximate entropy of brain network in the study of hemispheric differences, Entropy 22 (2020) 1–12 (Basel), doi:10.3390/E22111220.
[53] M. Hadra, A. Omidvarnia, M. Mesbah, Temporal complexity of EEG encodes human alertness, Physiol. Meas. 43 (2022), doi:10.1088/1361-6579/AC8F80.
[54] S.S. Taylor, N. Noor, I. Urits, A. Paladini, M.S. Sadhu, C. Gibb, T. Carlson, D. Myrcik, G. Varrassi, O. Viswanath, Complex regional pain syndrome: a comprehensive review, Pain Ther. 10 (2021) 875–892, doi:10.1007/S40122-021-00279-4.
[55] J.H. Zimering, M.R. Williams, M.E. Eiras, B.A. Fallon, E.L. Logigian, R.H. Dworkin, Acute and chronic pain associated with Lyme borreliosis: clinical characteristics and pathophysiologic mechanisms, Pain 155 (2014) 1435–1438, doi:10.1016/J.PAIN.2014.04.024.